Colloid and Polymer Science (2018) 296:483–494
https://doi.org/10.1007/s00396-018-4263-5

ORIGINAL CONTRIBUTION

Interactional behavior of surface active ionic liquid lauryl isoquinolinium bromide and anionic polyelectrolyte poly(4-styrenesulfonic acid-*co*-maleic acid) sodium salt in aqueous solution

Amalendu Pal[1] · Ritu Maan[1]

Received: 14 July 2017 / Revised: 21 December 2017 / Accepted: 3 January 2018 / Published online: 25 January 2018

Abstract
In the present study, we have reported a detailed assessment of interactional behavior between the surface active ionic liquid (SAIL) lauryl isoquinolinium bromide ([C_{12}iQuin][Br]) and anionic polyelectrolyte poly(4-styrenesulfonic acid-*co*-maleic acid) sodium salt (PSS-co-MA) in aqueous media. Various techniques such as surface tension, conductance, dynamic light scattering, and turbidity have been employed to get insight into interactions among [C_{12}iQuin][Br] and polyelectrolyte in the interfacial region. Then, surface parameters such as surface excess concentration (Γ_{cmc}), surface pressure at interface (Π_{cmc}), minimum area occupied by one molecule of SAIL at air–solvent interface (A_{min}), adsorption efficiency (pC_{20}), and surface tension at critical micelle concentration (cmc) (γ_{cmc}) have been calculated from tensiometric measurements. Further, thermodynamic parameters, i.e., standard enthalpy of micellization $\left(\Delta H_m^\circ\right)$, standard free energy of micellization (ΔG_m°), and standard entropy of micellization (ΔS_m°) have been evaluated. The size and shape of complexes formed among [C_{12}iQuin][Br] and polyelectrolyte have been characterized using DLS and turbidity measurements.

Keywords Polyelectrolyte–SAIL complex · Surface tension · Conductance · DLS · Turbidity

Introduction

The interestingly unusual properties of ionic liquids [1–6] give rise to applications of scientific and industrial interest such as cosmetics, paints, detergency, foods, drug delivery, coatings [7], high-performance capillary electrophoresis [8, 9], pharmaceuticals [10], bioscience, water and soil treatment, oil recovery [11], and nanotechnology [12]. It has been foreseen that ionic liquids hold a convincing potential in surfactant industry [13]. Additionally, ionic liquids having long alkyl chain groups are amphiphilic in nature and have been termed as surface active ionic liquids (SAILs). In addition to the properties of parent ionic liquid, SAILs possess enhanced surface activity as well as antimicrobial activity [14–16]. The interactions between similar charged surfactant and polyelectrolyte/polymer are rendered considerably absent or feeble. However, the obvious strong interactions exist among oppositely charged surfactant and polyelectrolyte owing to strong attractive electrical attraction. So these systems hold special attention from investigation point of view. The molecular structure plays an important role in deciding the properties of a particular ionic liquid and there has been a continuous ongoing effort dedicated to find out superior alternatives for a particular application. The various applications of SAILs in aqueous polyelectrolyte solutions rest upon the understanding of the complex interaction mechanism between SAILs and polyelectrolytes.

While studying the systems of oppositely charged surfactant and polyelectrolyte/polymer, expecting the strong attractive association is quite acceptable. However, repulsive interactions among charged parts of surfactant and charged parts of polyelectrolytes cannot be ignored and need special consideration. The interplay of electrostatic and hydrophobic interactions decides the micellization behavior of the respective system under investigation. The polymeric chains induce micelle formation. As micellization is the most significant characteristic of any surfactant solution, the knowledge of driving

✉ Amalendu Pal
palchem21@gmail.com

[1] Department of Chemistry, Kurukshetra University, Kurukshetra 136119, India

forces for micelle formation becomes essential, and for this sake, parameters such as free energy, enthalpy, and entropy of micellization have been calculated by applying the laws of thermodynamics.

Recently, the interaction of anionic polymer sodium polystyrene sulphonate (NaPSS) with cationic surface active ionic liquid based upon imidazolium, [$C_n$mim][Cl] (n = 10, 12, 14) [17] and [C_8mim][Br] [18], has been investigated by Mahajan et al. and our group respectively. Wei et al. [19] have also studied the interaction of aqueous 1-methyl-3-tetradecylimidazolium bromide ([C_{14}mim][Br]) with NaPSS through various methods. The interactions among 1-dodecyl-3-methylimidazolium bromide and sodium carboxymethylcellulose (NaCMC) have also been studied by Jie et al. [20]. A detailed discussion is available on the micellization behavior of pyridinium-based ionic liquids in aqueous solutions [14, 21–23]. Isoquinolinium compounds have been found to have superior biologically activity as compared to the pyridinium-based ILs and quaternary ammonium-based surfactants which opens the gateways to multitudinous applications in medical field [24]. Lauryl isoquinolinium bromide ([C_{12}iQuin][Br]) is a cationic surfactant having melting point 49 °C. There are not so many reports available on the isoquinolinium-based ionic liquids [25–30]. Zhang et al. [31] have made an effort to investigate the micellization of some of N-alkyisoquinolinium-based ionic liquids such as butyl isoquinolinium bromide ([C_4iQuin][Br]), octylisoquinolinium bromide ([C_8iQuin][Br]), and [C_{12}iQuin][Br] in aqueous solution by employing the techniques such as surface tension, electrical conductivity, and ^{1}H NMR measurements. We have made a keen effort to investigate the underlying interactions among [C_{12}iQuin][Br] and aqueous solutions of anionic polyelectrolyte poly (acrylic acid sodium salt) (NaPAA) in our previous communication [A. Pal, R. Maan, Journal of surfactants and detergents, Under Revision, 2017]. With the progressive addition of SAIL to the aqueous solutions of polyelectrolyte, various transitions have been observed. Initially, there has been the formation of [C_{12}iQuin][Br]–NaPAA complex resulted due to electrostatic attractive interactions among them followed by precipitation, and finally, cmc is achieved. The results obtained from various techniques complement each other very well. The results obtained from DLS and turbidity measurements show that size of micelle-like aggregates first decreases and then increases in the presence of polyelectrolyte. The binding isotherms obtained using isothermal titration calorimetry (ITC) show the concentration dependence as well as the highly co-operative nature of interactions corresponding to formation of polyelectrolyte–SAIL complexes. Now, we have extended our investigation on the surface properties of [C_{12}iQuin][Br] in aqueous solution of an oppositely charged polyelectrolyte poly(4-styrenesulfonic acid-*co*-maleic acid) sodium salt (PSS-co-MA) by using surface tension, electrical conductivity, dynamic light scattering, and turbidity measurements. There is no report available on the interactional behavior of ILs such as [C_{12}iQuin][Br] and PSS-co-MA in aqueous media. Altogether, these provide an understanding of the role of various interactions prominent in our current system under study. The schematic of the present work has been presented in Scheme 1.

Experimental

Materials

1-Bromododacane (> 98%), poly(4-styrenesulfonic acid-*co*-maleic acid) sodium salt (PSS-co-MA) (M_w ~20,000, 1:1 4-styrenesulfonic acid:maleic acid mole ratio), and isoquinoline (97%) were purchased from Sigma-Aldrich. Methanol (99%) was bought from Rankem. All aqueous solutions have been prepared using Millipore-grade water. The specific conductivity and surface tension of Millipore-grade water were measured and were found to be 3 μS cm^{-1} and 71 mN m^{-1} respectively. The ionic liquid [C_{12}iQuin][Br] has been synthesized and purified in laboratory followed by drying under reduced pressure. ^{1}H NMR technique has been used to verify the purity of [C_{12}iQuin][Br]. The detailed information of chemicals used in the present study has been provided in Table 1.

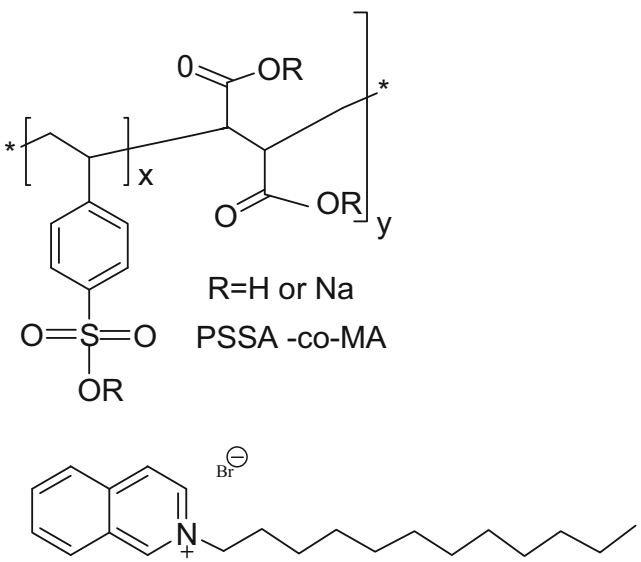

Scheme 1 Chemical structure of ionic liquid lauryl isoquinolinium bromide ([C_{12}iQuin][Br]) and polyelectrolyte poly(4-styrenesulfonic acid-*co*-maleic acid) sodium salt (PSS-co-MA)

Table 1 The specification of chemicals

Chemical name	CAS No.	Source	Purity (mass %)
Isoquinoline	119-65-3	Sigma-Aldrich, USA	97%
1-Bromododecane	143-15-7	Sigma-Aldrich, USA	> 98%
Dichloromethane	75-09-2	Sigma-Aldrich, USA	–
Poly(4-styrenesulfonic acid-*co*-maleic acid) sodium salt (M_w ~20,000)	68037-40-1	Sigma-Aldrich, USA	–

Synthesis of lauryl isoquinolinium bromide

A particular amount of both of the reactants, i.e., isoquinoline and alkyl bromide, were weighed and added to a 250-mL round-bottomed flask along with solvent acetonitrile under nitrogen atmosphere. The reaction mixture was heated to reflux for 2 h. Then, dichloromethane was added to the crude product obtained after refluxing followed by the addition of activated carbon to achieve decolorization. Finally, the red colored thick oil was obtained which was allowed to cool at room temperature and several washings with n-hexane were performed in order to achieve recrystallization and remove any unreacted reagents. Then, [C_{12}iQuin][Br] was kept under vacuum for 3 days to ensure the elimination of any solvent residue. The moisture content was found to be less than 0.02 wt% from Karl-Fischer titration method. The structure of [C_{12}iQuin][Br] was confirmed by analyzing its ^{1}H NMR spectra.

The NMR details of corresponding protons for [C_{12}iQuin][Br] are given as follows: DMSO-d6 0.85(t,3H), 1.22(m,20H), 4.76(t,2H), 8.28(t,1H), 8.40(t,1H), 8.53(d,1H), 8.65(d,1H), 8.89(d,1H), and 10.23(S,1H).

Instruments and methods

All aqueous solutions have been prepared with Millipore-grade water. A & D co limited electronic balance (Japan, model GR-202) has been used to weigh the chemicals and it has an accuracy of 0.01 mg.

Tensiometry

Surface tension measurements were performed out at 298.15 K by a Data Physics, Model DCAT-II automated tensiometer which employs the Wilhelmy plate method. The successive additions of IL into the aqueous polyelectrolyte solution were made by volume. Then, the solution was stirred for few minutes with an aim to achieve complete solubilization. After stirring, the solutions were allowed to rest for few minutes to equilibrate. Three readings were noted and they were accurate within ± 0.02 mN m^{-1}. The Julabo water thermostat was used in order to control temperature with an uncertainty of 0.01 K.

Conductivity measurements

A digital conductivity meter CM-183 microprocessor-based EC-TDS analyzer with ATC probe has been used to measure electrical conductivities in solution. The conductivity cell having electrodes made up of platinium metal and cell constant 1.003 cm^{-1} was purchased from Elico Ltd., India. It was calibrated with aqueous KCl solutions (0.01–1.0 mol kg^{-1}) before any experimental measurement was made. The measurements were performed in a double-walled flow dilution cell which has been jacket by water and it had an uncertainty of 0.01 K at 298.15 K. Three readings were noted for every particular concentration, and finally, mean values were considered. The uncertainty in the electrical conductivity measurements was less than 4%.

Dynamic light scattering and turbiditimetry

DLS measurements were carried out with the help of NaBiTecSpectro-Size300 light-scattering apparatus (NaBiTec, Germany) with a He–Ne laser source (633 nm, 4 mW) at 298.15 K. A membrane filter of 0.45 μm pore size was used to filter [C_{12}iQuin][Br]–NaPAA solutions of appropriate concentrations into quartz cell which was previously rinsed with filtered water. The measurements were performed at controlled temperature within accuracy of 0.1 K. The laser light from source falls upon the cell containing sample and the scattered light signal is obtained at a scattering angle of 90°. The instrument has inbuilt CONTIN algorithm which was used to evaluate DLS data.

The turbiditimetric measurements of the solutions were performed using (Eutech TN-100) turbiditimeter. [C_{12}iQuin][Br]–NaPAA solutions of appropriate concentrations were prepared followed by stirring for few minutes. Then, the samples were allowed to equilibrate for approximately 5 min, and then, the measurement was made.

Results and discussion

The complex formation among [C_{12}iQuin][Br] and PSS-co-MA in aqueous media at various concentration of PSS-co-MA has been studied using different techniques such as surface tension, conductance, dynamic light scattering, and turbiditimetry.

Tensiometry

Surfactants decrease the interfacial tension between the phases. The addition of polymer to surfactant solution generally improves the surface activity which depends upon the concentration of both the surfactant and polymer. As the surfactant solution of a particular concentration is added to the aqueous solution, the surface tension starts decreasing up to a point, typically called as cmc, after which the surface tension does not decrease further and becomes fairly constant. Beyond this point, all the surfactant added to the solution forms micelles. However, while considering the solutions of surfactant and polyelectrolytes/polymers, the scenario is not that straightforward. In these systems, we observe four distinct characteristic concentrations where the surface tension changes quite sharply corresponding to the progressive formation of SAIL–polyelectrolyte complex (c_1), critical aggregation concentration (cac), critical saturation concentration (c_s), and critical micelle concentration (cmc) which result from strong hydrophobic and electrostatic interactions. The interactions among surfactants and polyelectrolytes originate from hydrophobic and electrostatic interactions [32]. The association of surfactant to polymer is a co-operative phenomenon [33]. When the surfactant ([C_{12}iquin][Br]) solution has been added to the aqueous polyelectrolyte PSS-co-MA solution, the surface tension values start decreasing at concentration C_1 which corresponds to the adsorption of surfactant monomers at the PSS-co-MA surface. Initially, in the dilute region, only a small change in surface tension is noticed. Further, as the concentration of surfactant is increased, appearance of another hump corresponds to the cac which refers to the onset of association of surfactant monomers to the binding sites available on the chains of the polymer and formation of surface-active PSS-co-MA–[C_{12}iQuin][Br] aggregates. Further, beyond this point, co-operative binding of SAIL and polyelectrolyte results originated from the electrostatic binding followed by stabilization through hydrophobic interactions among SAIL's tails. During this phenomenon, SAIL ion replaces the counter ion of polyelectrolyte and a neutral ion pair is formed at the binding site. It leads to precipitation which is usually observed in the oppositely charged polyelectrolyte–SAIL systems [34]. As we proceed further, another characteristic transition is approached which means c_s. It means that the polyelectrolyte chains have become saturated with the surfactant monomers and no more free binding sites are available for surfactant monomers followed by cmc beyond which all the surfactant added forms free micelles into the solution. Once the cmc has been reached, no further decrease in surface tension has been observed indicating that polyelectrolyte surface has been fully occupied with surfactant monomers.

Tensiometric profiles of [C_{12}iQuin][Br] in different concentrations of PSS-co-MA (0, 0.005, 0.0075, and 0.01 g/L PSS-co-MA) have been plotted in Fig. 1. We have studied the interactions at lower concentrations as compared to

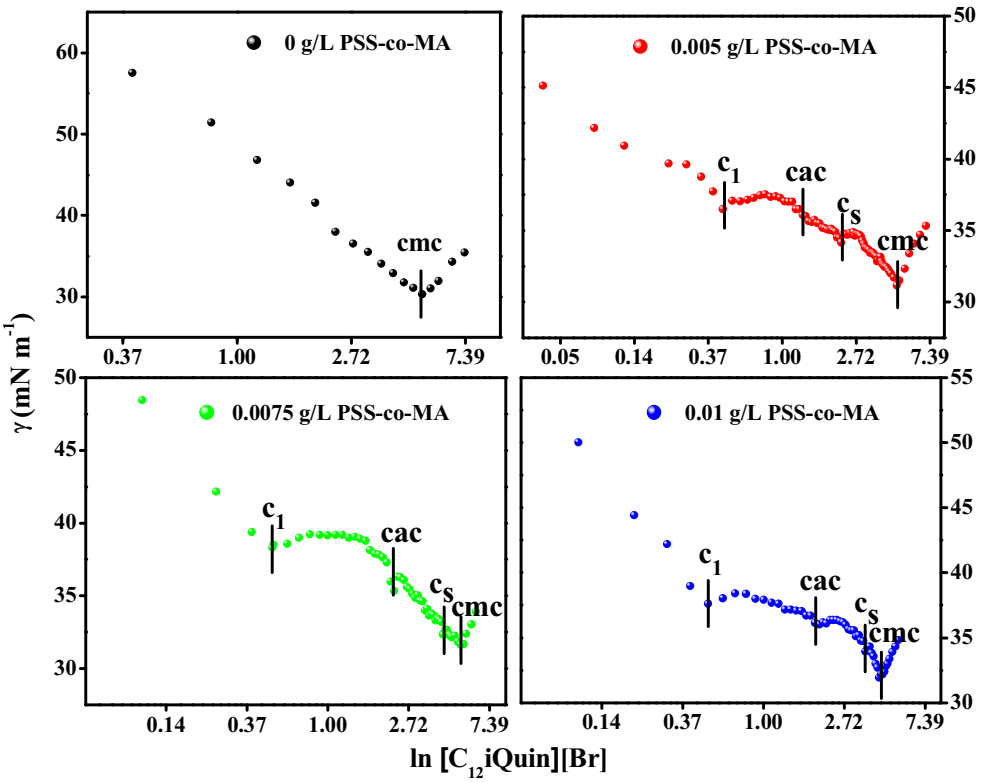

Fig. 1 Surface tension of aqueous solutions of [C_{12}iQuin][Br] and PSS-co-MA as a function of added [C_{12}iQuin][Br] in the absence (●) 0 g/L and presence of different concentrations (●) 0.005 g/L, (●) 0.0075 g/L, and (●) 0.01 g/L of PSS-co-MA at temperature 298.15 K

[C_{12}iQuin][Br]–NaPAA system because of higher turbidity levels at higher concentrations were observed. For pure [C_{12}iQuin][Br], the value of surface tension gradually decreases with the increase in concentration of SAIL until a knap regime, beyond which surface tension does not decrease further. All these characteristic interaction concentrations have been tabulated in Table 2. From Fig. 1 and Table 2, it is observed that the cmc has decreased with the addition of surfactant to the 0.005 g/L PSS-co-MAA solution which is a result of synergistic effect [35] resulted by strong electrostatic attractive interactions among the head groups of SAIL and polyelectrolyte. This phenomenon exists at a very low concentration of surfactant when even pure surfactant is incapable of getting adsorbed at the surface of the solution. The solvency of the backbone of polymer affects the structural aspects of the SAIL–polyelectrolyte complex. Typically, the polymers with hydrophobic tails do not stay around the head group region; rather, they penetrate into the miceller core and expand the hydrophobic moiety which decreases the cmc. However, the cmc value increases upon increasing the concentration of polyelectrolyte from 0.005 to 0.0075 g/L PSS-co-MAA solution and the same trend has been noticed by conductance measurements as well. The hydrophobic interactions override over electrostatic attractions between oppositely charged SAIL and polyelectrolyte due to which SAIL monomers have been stabilized leading to micellization at relatively higher concentration of polyelectrolyte. As we increase the concentration of polyelectrolyte from 0.0075 to 0.01 g/L PSS-co-MAA solution, the cmc again decreases.

Table 2 The various characteristic interaction concentrations c_1, cac, c_s, and cmc (mmol L^{-1}) observed from tensiometry and conductometry of [C_{12}iQuin][Br] in the absence and presence of the polyelectrolyte PSS-co-MA at 298.15 K

[PSS-co-MA] (g/L)		Tensiometry	Conductometry
0.0	cmc	5.05	5.22
0.005	c_1	0.45	1.02
	cac	2.23	2.12
	c_s	3.62	–
	cmc	4.73	4.38
0.0075	c_1	0.50	0.63
	cac	2.26	2.34
	c_s	4.13	–
	cmc	5.13	5.08
0.01	c_1	0.50	0.54
	cac	1.97	2.01
	c_s	3.47	–
	cmc	4.18	4.34

Uncertainties are s (conc. of PSS-co-MA) = $\pm 1 \times 10^{-3}$ g/L, s $(cmc)_{S.T.}$ = $\pm 2 \times 10^{-5}$ mol L^{-1}, s $(cmc)_{cond.}$ = $\pm 1 \times 10^{-5}$ mol L^{-1}, s (T) = $\pm 1 \times 10^{-2}$ K, and $s(p)$ = ± 2 kPa

Some other intermediate concentrations of the polyelectrolyte have been measured repeatedly in order to clarify the disturbance of the general tendency by the probe with 0.0075 g/L PSS-co-MA at the studied temperatures. We observed that the cmc has been found to decrease with increase in concentration but increases at 0.0075 g/L of PSS-co-MA and then finally decreases again as we increase the concentration further to 0.01 g/L (Table 3). The increase in cmc values for [C_{12}iQuin][Br] in the presence of 0.0075 g/L PSS-co-MA may be due to partial shifting of interacting [C_{12}iQuin][Br] and polyelectrolyte molecules from the surface towards the bulk for aggregate formation. It means that there is a competitive formation of surface polyelectrolyte/SAIL complexes and bulk polyelectrolyte/SAIL complexes. The difference in behavior of the polyelectrolyte–surfactant samples arises owing to modifications in the surface and bulk properties of the system. In general, the increase in cmc values with increase in polymer concentration has been observed by Cervantes-Martínez A and Pandey et al. [36, 37]. They reported that interfacial area expansion, surfactant monomer diffusion, and breakdown of micelles are responsible for this phenomenon. Here, there is competitive in this phenomenon that opposes micellization and hence increases the cmc at 0.0075 g/L of PSS-co-MA.

We have obtained different trend for the oppositely charged system [C_{12}iQuin][Br] and NaPAA. The cmc values decrease upon increasing the concentration of polyelectrolyte up to 0.01 g/L NaPAA but different trend has been noted as we increase the concentration further from 0.01 to 0.025 g/L NaPAA.

Further, from the tensiometric profile, the various surface parameters have been determined by using Gibbs equation such as surface excess concentration (Γ_{max}), surface pressure at the interface (π_{cmc}), minimum area at air–solvent interface (A_{min}) covered by single monomer of SAIL, and surface tension at cmc (γ_{cmc}) [38] and their corresponding values have been provided in Table 4.

The Γ_{max} is usually calculated through the measurement of adsorption of SAIL in the air–liquid interface obtained by using the following equation [39]:

$$\frac{d\gamma}{d\ln C_T} = -nRT\Gamma_{max} \quad (1)$$

where γ is surface tension, R is universal gas constant, T is the temperature, n represents the number of ions formed in solution, and C_T denotes SAIL's concentration at a particular temperature. The minimum area occupied by the SAIL, A_{min}, has been calculated from [40]:

$$A_{min} = \frac{10^{20}}{N_A \times \Gamma_{max}} \quad (2)$$

where N_A is Avogadro's number. The values of Γ_{max} and A_{min}

Table 3 The values of critical micelle concentration (cmc), degree of dissociation (α), free energy of micellization (ΔG_m°), enthalpy of micellization (ΔH_m°), and entropy of micellization (ΔS_m°) of aqueous [C_{12}iQuin][Br] solutions in different concentrations of PSS-co-MA at different temperatures

PSS-co-MA (g/L)	cmc (mM)	α	(ΔH_m°) (kJ mol^{-1})	(ΔG_m°) (kJ mol^{-1})	(ΔS_m°) (JK^{-1} mol^{-1})
T = 298.15 K					
0.0	5.22	0.375	− 12.13	− 37.35	84.58
0.005	4.38	0.377	− 10.02	− 38.01	93.88
0.0075	5.08	0.386	− 5.29	− 37.21	107.05
0.01	4.36	0.372	− 10.72	− 38.14	91.99
T = 308.15 K					
0.0	5.39	0.387	− 12.24	− 38.18	84.18
0.005	4.71	0.390	− 10.59	− 38.67	91.12
0.0075	4.92	0.399	− 6.31	− 38.27	103.74
0.01	4.47	0.383	− 10.21	− 39.05	93.60
T = 318.15 K					
0.0	5.63	0.396	− 13.04	− 39.02	81.66
0.005	4.91	0.397	− 15.82	− 39.57	74.67
0.0075	4.85	0.410	− 5.93	− 39.30	104.90
0.01	4.58	0.393	− 11.99	− 39.98	87.98

Uncertainties are s (conc. of PSS-co-MA) = ± 1 × 10^{-3} g/L, s (cmc)$_{cond.}$ = ± 1 × 10^{-5} mol L^{-1}, s (ΔG_m°) = ± 0.02 kJ mol^{-1}, s (ΔH_m°) = ± 0.01 kJ mol^{-1}, s(ΔS_m°) = ± 0.02 kJ mol^{-1}, s (T) = ± 1 × 10^{-2} K, and s (p) = ± 2 kPa

have been found to follow the opposite trend. For [C_{12}iQuin][Br]–PSS-co-MAA system in aqueous solution of different concentrations of PSS-co-MAA, Γ_{max} decreases and A_{min} increases (with an exception of 0.0075 g/L PSS-co-MAA) which suggests that there exists higher concentration of SAIL molecules at the air–aqueous interface. The increasing values of A_{min} indicate that packing density increases with increasing the polyelectrolyte concentration at the interface.

The pC_{20} is an important surface parameter, which is known as the adsorption efficiency and that can be obtained from the following equation:

$$pC_{20} = -\log C_{20} \tag{3}$$

Table 4 The surface parameters, i.e., surface tension at cmc (γ_{cmc}), effective surface tension reduction (π_{cmc}), surface excess (Γ_{max}), minimum area per molecule (A_{min}), and adsorption efficiency (pC_{20}), of [C_{12}iQuin][Br] and [C_{12}iQuin][Br] at different PSS-co-MA concentrations

[[PSS-co-MA] (g/L)	γ_{cmc} (mN m^{-1})	π_{cmc} (mN m^{-1})	$\Gamma_{max} \times 10^6$ (mol m^{-2})	A_{min} (nm^2)	pC_{20}
T (298.15 K)					
0.0	30.50	31.15	1.36	1.22	0.85
0.005	31.26	31.15	0.13	13.24	1.84
0.0075	31.71	31.61	0.20	8.23	0.26
0.01	31.99	31.88	0.03	52.10	3.13

Uncertainties are s (conc. of PSS-co-MA) = ± 1 × 10^{-3} g/L, s (π_{cmc}) = ± 0.2 mM m^{-1}, s (Γ_{max}) = ± 0.03 × 10^{-6} mol m^{-2}, s (A_{min}) = ± 0.02 nm^2,, s (T) = ± 1 × 10^{-2} K, and s (p) = ± 2 kPa

where C_{20} is the SAIL concentration which decreases the value of γ for pure water by 20 mN m^{-1}. This is the lowest concentration which is required to lead saturation of the surface adsorption. The values of pC_{20} have been found to increase for [C_{12}iQuin][Br]–PSS-co-MAA system with the increase in the concentration of PSS-co-MAA (except for 0.0075 g/L PSS-co-MAA) which indicates that the adsorption efficiency has increased at the air–aqueous interface upon increasing the concentration of polyelectrolyte for [C_{12}iQuin][Br]–PSS-co-MAA system. The substantial decrease in the value of C_{20} at 0.0075 g/L PSS-co-MA indicates the decrease in the adsorption efficiency with increase in concentration from 0.005 to 0.0075 g/L PSS-co-MA. It suggests that at 0.0075 g/L PSS-co-MA, there is a decrease in the surface activity of SAIL.

Further, a parameter π_{cmc}, the comparative effectiveness of SAIL molecule, has been estimated by surface pressure at cmc. That has been calculated using the following equation [40]:

$$\pi_{cmc} = \gamma_0 - \gamma_{cmc} \tag{4}$$

where γ_{cmc} is the surface tension at cmc for a solution of particular concentration and γ_0 is the surface tension of pure solvent. From the data, it shows that overall values of π_{cmc} have been found to decrease with an increase in the concentration of PSS-co-MA, which implies that the efficiency of SAIL in reducing the value of surface tension decreases in existence of polyelectrolyte. However, for 0.0075 g/L PSS-

co-MA, the value of π_{cmc} has decreased which is in accordance with the reason stated above.

Conductance measurements

The experimental electrical conductivities of aqueous [C_{12}iQuin][Br] solutions in the absence and presence PSS-co-MA in different concentrations (0, 0.005, 0.0075, and 0.01 g/L PSS-co-MA) have been presented in Fig. 2. The values of cmc and various parameters have been listed in Table 2. In the electrical conductivity versus concentration plots, two straight lines have been obtained. These lines have been found to have different slopes for which micelle formation can be held responsible. The cmc value has been assigned to the point of intersection of these two tangential lines. The conductometric profiles of the systems studied show a decrease in the values of cmc of [C_{12}iQuin][Br] after the addition of the polyelectrolyte PSS-co-MA. It means that the electrostatic attractive interaction between the positively charged head group of [C_{12}iQuin][Br] and negatively charged groups on the chain of polyelectrolyte is dominant over the hydrophobic interactions existing among the hydrophobic tail PSS of anionic polyelectrolyte poly(4-styrenesulfonic acid-*co*-maleic acid) sodium salt and docecyl chain of lauryl isoquinolium bromide. These interactions give rise to micelle formation at a comparatively lower concentration of SAIL.

The specific conductance (κ) of aqueous [C_{12}iQuin][Br] solutions in the presence of different concentrations of PSS-co-MAA at different temperatures has been depicted in Fig. 3. From Table 3, it is clear that the cmc initially decreased upon addition of surfactant to the lower concentrations of PSS-co-MA due to micelle formation. The electrostatic interactions among oppositely charged SAIL and polyelectrolytes reduce the repulsion among head groups at micellar surface which leads to early micelle formation as compared to pure SAIL system. As the oppositely charged groups on polyelectrolyte chain get attracted to the oppositely charged head groups of SAIL, there is effective screening of the repulsive electrostatic interaction and the head groups of SAIL are closely packed up. It effectively facilitates the growth of micelle. However, upon increasing the concentration to 0.0075 g/L PSS-co-MA, an increase in cmc has been noticed. The steric interactions among the bulky head groups of SAIL prevail and stabilization of individual surfactant monomers via hydrophobic interactions can be accounted for this phenomenon. However, further increasing the concentration to 0.01 g/L PSS-co-MA, again, a decrease in cmc has been observed which indicates the early stabilization of SAIL.

The ratio of slopes of pre and post miceller region in the conductance versus concentration profile [41–44] provides the degree of counter-ion dissociation (α). In the conductivity profiles, a break has been observed in the high SAIL concentration which is around cac in the surface tension trends followed by cmc. The redissolution leading to restricted movement of counter ions can be hold accountable for the slow increase in conductance after cmc. Finally, on further addition of SAIL, more and more SAIL molecules adsorb on the backbone of polyelectrolyte leading to enhanced positive charge on the polyelectrolyte. If the concentration of polyelectrolyte

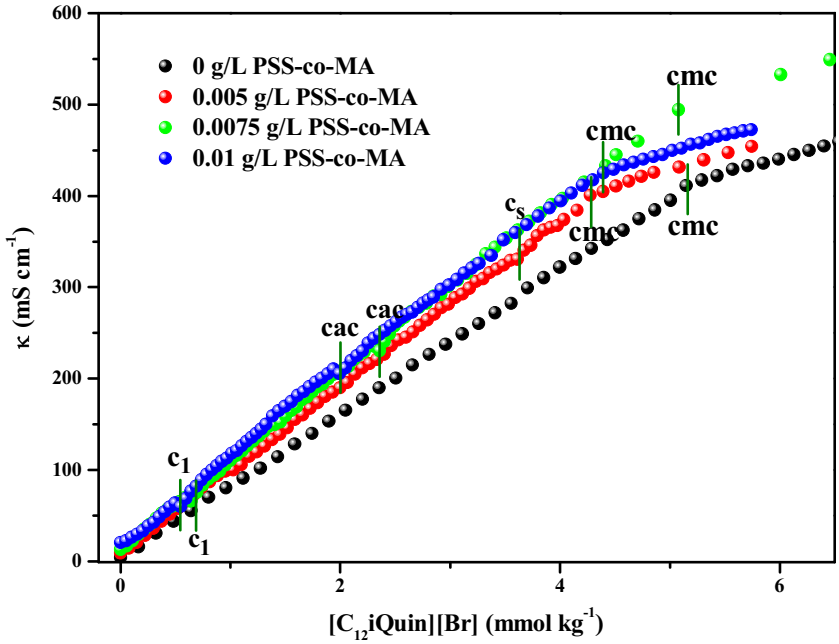

Fig. 2 Specific conductance (κ) of aqueous [C_{12}iQuin][Br] solutions in the absence (●) 0 g/L and presence of different concentrations (●) 0.005 g/L, (●) 0.0075 g/L, and (●) 0.01 g/L of PSS-co-MA at temperature 298.15 K

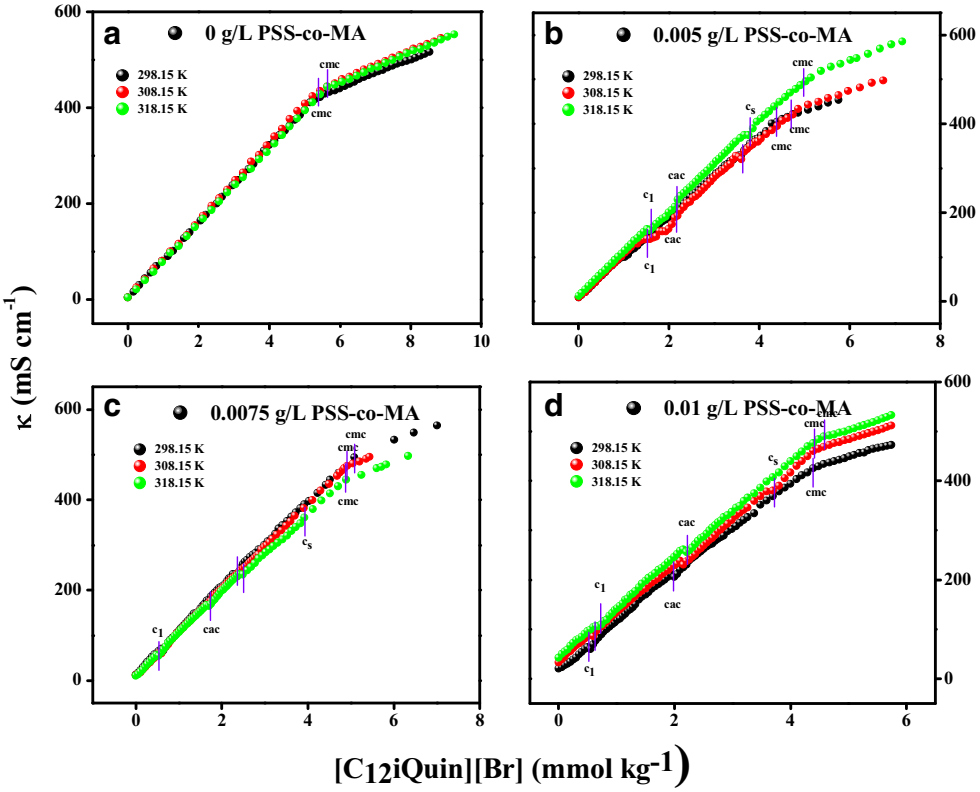

Fig. 3 Specific conductance (κ) of aqueous [C_{12}iQuin][Br] solutions in the presence of different concentrations of PSS-co-MA **a** 0 g/L, **b** 0.005 g/L, **c** 0.0075 g/L, and **d** 0.01 g/L PSS-co-MA at different temperatures (●) 288.15 K, (●) 298.15 K, and (●) 308.15 K

is increased, values of cmc of systems under investigation decrease except at the intermediate concentration for the reason mentioned in the previous section. The cmc variation with temperature depends upon many factors [45]. Figure 3 shows an increase in cmc with increase in temperature for 0, 0.005, and 0.01 g/L PSS-co-MA and a decrease for 0.0075 g/L PSS-co-MA. The cmc variation with temperature has been resulted from the unfavorable circumstances for the micelle formation originated from the destruction of water structure around the hydrophobic groups. However, the decrease in cmc with increase in temperature has been observed for 0.0075 g/L PSS-co-MA which may be accounted to the decreased hydration of hydrophilic groups.

Various thermodynamic parameters of micellization have been calculated for SAIL–polyelectrolyte system of current interest using the temperature dependence of cmc. The standard Gibbs free energy (ΔG_m°) of micellization for the SAIL–polyelectrolyte all the systems were calculated using the following equation [46]:

$$\Delta G_m^\circ = (2-\alpha)RT\ln X_{cmc} \tag{5}$$

where T is the temperature of the system, R represents universal gas constant, and X_{cmc} is cmc that has been obtained from the electrical conductivity versus concentration plots and has been expressed in mole fraction.

The enthalpy of micellization (ΔH_m°) has been obtained by applying van't Hoff equation [42]:

$$\Delta H_m^\circ = -RT^2\left[(2-\alpha)\frac{d\ln X_{cmc}}{dT} + \ln X_{cmc}\frac{d(1-\alpha)}{dT}\right] \tag{6}$$

Further, entropy of micellization, (ΔS_m°) has been calculated using the following equation [46]:

$$\Delta S_m^\circ = \frac{\Delta H_m^\circ - \Delta G_m^\circ}{T} \tag{7}$$

By using the provided equations, the thermodynamic variables have been calculated and reported in Table 3. The changes in different parameters have been observed with change in polyelectrolyte concentration and they collectively direct towards major important phenomenon occurring into SAIL–polyelectrolyte aqueous solutions. The values of ΔS_m° have been found positive indicating that the micellization process is driven by entropy. The values of ΔS_m° are greater in the presence of polyelectrolyte. There exists a highly ordered structure of water around the hydrocarbon chain of surfactant monomers. When these monomers associate into micelles, this ordered structure of water breaks followed by releasing

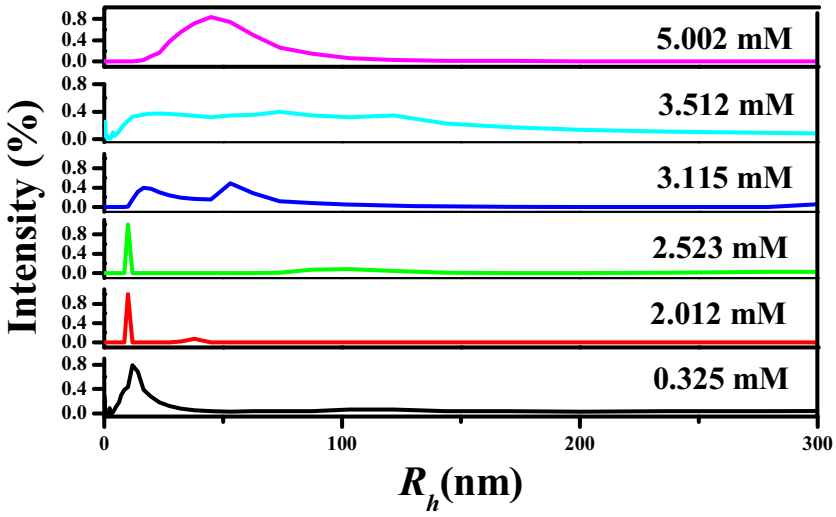

Fig. 4 Distribution of the hydrodynamic diameter R_h for 0.01 g/L PSS-co-MA solution in the presence of different [C_{12}iQuin][Br] concentrations at temperature 298.15 K

of water molecules and this accounts for higher entropic states of the system. The ΔH°_{m} values have been found negative for all the concentrations of PSS-co-MA indicating that micellization process is exothermic. With the increase in polyelectrolyte concentration, the overall ΔH°_{m} decreases pointing that less heat has been evolved with increase in concentration of PSS-co-MA. It is inferred that the enthalpy change contribution is lesser than the entropy-driven phenomenon during micellization process at all concentrations. Also, ΔH°_{m} values decrease with increase in concentration but increase with temperature which means that the process is more exothermic at lower polyelectrolyte concentration and higher temperature. We conclude that, at lower surfactant concentration or at higher polyelectrolyte concentration, the electrostatic interactions are dominant due to binding of [C12iQuin][Br] monomers to the PSS-co-MA chain. As the [C12iQuin][Br] concentration increases, the interaction between [C12iQuin][Br] and PSS-co-MA decreases leading to the formation of four characteristic surfactant concentrations.

The tendency to acquire minimum free energy has been considered as the driving force for the micellization process. The values of ΔG°_{m} have been found negative indicating that the micellization is a spontaneous process. The values of ΔG°_{m} become more negative upon increasing the concentration of PSS-co-MA indicating that the process has become more spontaneous and the SAIL's efficiency has increased in the presence of PSS-co-MA (except at 0.0075 g/L PSS-co-MA). Also, for our previous system [C12iQuin][Br] and NaPAA, it was inferred that the enthalpy change contribution was lesser and the it was entropy-driven phenomenon. The values of ΔG°_{m} became more negative upon increasing the concentration of NaPAA indicating that the process was more spontaneous. The efficiency of SAIL was improved in the presence of NaPAA.

Dynamic light scattering and turbiditimery

Dynamic light scattering measurements (also termed as photon correlation spectroscopy) were performed to determine the hydrodynamic size and type of the self-assembled aggregates of [C_{12}iQuin][Br] in aqueous medium in the presence of 0.01 g/L PSS-co-MA solution to get insight into the distribution of size along with change in concentration. It provides the time dependence of fluctuations in the intensity of light with the help of which diffusion coefficient, and finally, the miceller hydrodynamic radius has been obtained. The hydrodynamic radii, R_h, of the self-assembled structures measured from DLS have been presented in Fig. 4. Upon the addition of SAIL in the concentration range below c_1, SAIL monomers just start to chains of polymer because of electrostatic attraction as observed in the electrical conductivities as well as tensiometric measurements

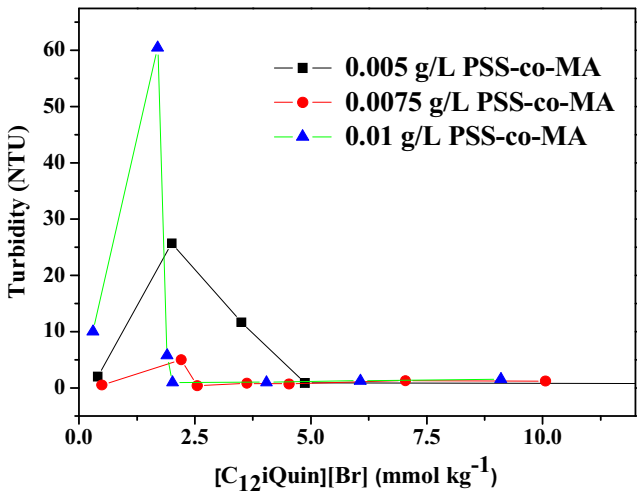

Fig. 5 Turbiditimetric profiles of [C_{12}iQuin][Br] in the presence of different concentrations (●) 0.005 g/L, (●) 0.0075 g/L, and (●) 0.01 g/L of PSS-co-MA at temperature 298.15 K

at c_1 and two different peaks are observed in DLS measurements. The two different peaks correspond to both the polyelectrolyte monomer and multimers. In the beginning, there is a small, narrow peak in the vicinity of large and prominent first peak which refers to the starting of formation of multimers. Later, with the increase in the surfactant concentration, the second peak becomes significantly broader showing the existence of polyelectrolyte and SAIL complex. The first peak with smaller hydrodynamic radii refers to the soluble complex formed between SAIL and polyelectrolyte in the diluted equilibrium solution while the latter with larger hydrodynamic radii stands for the insoluble aggregates of SAIL and polyelectrolyte. If the surfactant addition is continued further, SAIL shows a decrease in R_h which is due to the compactness of structure of PSS-co-MA–[C_{12}iQuin][Br] complex as the polymeric chains coil up caused by the approaching hydrophobic parts of the SAIL towards each other. This creates aggregates of bounded SAIL molecules to polyelectrolyte chain. Finally, for [C_{12}iQuin][Br], at a concentration exceeding cmc, hydrodynamic radii shrink due to existing polyelectrolyte–SAIL complex. The same behavior has been noted for [C_{12}iQuin][Br] and NaPAA systems..

An attempt has also been made to get insight into the size of complexes formed among [C12iQuin][Br] and PSS-co-MA in the concentration range of interest using turbiditimetry. The change in turbidity of SAIL in different concentrations of aqueous polyelectrolyte solutions has been depicted in Fig. 5. The turbidity initially increases with increase in the concentration of SAIL, and then, precipitation is observed. At surfactant concentrations exceeding cac, the turbidity sharply decreases and becomes roughly constant which is due to redissolution of precipitates. We have achieved higher turbidity levels for the current systems as compared to [C_{12}iQuin][Br] and NaPAA system studied recently.

Conclusion

The studies related to the micellization behavior of a cationic surfactant [C_{12}iQuin][Br] in aqueous solutions of an oppositely charged polyelectrolyte PS-co-MA have been performed by using surface tension, conductance, dynamic light scattering, and turbidity measurements. The cmc obtained from various techniques have been found to be well correlated with each other. We found that the electrostatic interactions have been sufficient enough to form strong complexes between the polyelectrolyte and the oppositely charged SAIL. The binding has been favored by the large electrostatic attraction in the current systems and this association process is spontaneous and exothermic. The binding occurred at very low free surfactant concentration. The cmc overall has decreased owing to electrostatic attractive interactions prevailing in the systems of current interest except at intermediate concentration of polyelectrolyte. This is due to overriding of hydrophobic interactions among the hydrocarbon tails of the [C_{12}iQuin][Br] and PSS-co-MA interacting altogether in aqueous solution. The steric constraints among SAIL head groups and polyelectrolyte segment are present on the miceller interface. These tend to immobilize the micelle which is responsible for the observed trend. Later, the self-assembled structures were characterized with DLS and turbidity. The hydrodynamic radii initially increased as the binding between SAIL and polyelectrolyte chains initiated. Then, it was followed by two different peaks related to monomers as well as multimers. Finally, the hydrodynamic radii shrink due to the presence of SAIL–polyelectrolyte complex. The turbidity initially decreased after cac due to precipitation and then roughly became constant because the precipitates were redissolved [32, 47].

Acknowledgements Authors thank Mr. Praveen Singh Gehlot, Research Scholar at CSIR-CSMCRI, Bhavnagar for assisting in experimental measurements.

Funding This study was funded by Council of Scientific and Industrial Research (CSIR), Government of India (Grant No. 21(1005)/15/EMR-II) through Emeritus Scientist grant to Prof. A. Pal.

Compliance with ethical standards

Conflict of interest The authors declare that they have no conflict of interest.

References

1. Welton T (1999) Room-temperature ionic liquids. Solvents for synthesis and catalysis. Chem Rev 99(8):2071–2084. https://doi.org/10.1021/cr980032t
2. Dupont J, de Souza RF, Suarez PAZ (2002) Ionic liquid (molten salt) phase organometallic catalysis. Chem Rev 102(10):3667–3692. https://doi.org/10.1021/cr010338r
3. Wasserscheid P (2006) Chemistry: volatile times for ionic liquids. Nature 439(7078):797. https://doi.org/10.1038/439797a
4. Seddon KR (2003) Ionic liquids: a taste of the future. Nature 2:36–365
5. Meli L, Lodge TP (2009) Equilibrium vs metastability: high-temperature annealing of spherical block copolymer micelles in an ionic liquid. Macromolecules 42(3):580–583. https://doi.org/10.1021/ma802020a
6. Solinas M, Pfaltz A, Cozzi PG, Leitner W (2004) Enantioselective hydrogenation of imines in ionic liquid/carbon dioxide media. J Am Chem Soc 126(49):16142–16147. https://doi.org/10.1021/ja046129g
7. Polymer-surfactant systems (1998) In: JCT K (ed) Surfactant science series. Marcel Dekker, New York
8. Benedek K, Thiede S (1994) High-performance capillary electrophoresis of proteins using sodium dodecyl sulfate-poly(ethylene oxide). J Chromatogr A 676(1):209–217. https://doi.org/10.1016/0021-9673(94)80462-1
9. Tseng WL, Lin YW, Chang HT, Tseng WL, Lin YW, Chang HT (2002) Improved separation of microheterogeneities and isoforms of proteins by capillary electrophoresis using segmental filling with SDS and PEO in the background electrolyte. Anal Chem 74(18):4828–4834. https://doi.org/10.1021/ac020140m

10. Yoshida K, Dubin PL (1999) Complex formation between polyacrylic acid and cationic/nonionic mixed micelles: effect of pH on electrostatic interaction and hydrogen bonding. Colloids Surf A Physicochem Eng Asp 147(1–2):161–167. https://doi.org/10.1016/S0927-7757(98)00747-X
11. Goddard ED, Ananthapadmanabhan KP (1993) Eds. Interactions of surfactants with polymers and proteins. CRC Press Boca Raton FL Chapter 4
12. Leonov AP, Zheng J, Clogston JD, Stern ST, Patri AK, Wei A (2008) Detoxification of gold nanorods by treatment with polystyrenesulfonate. ACS Nano 2(12):2481–2488V. https://doi.org/10.1021/nn800466c
13. Blesic M, Lopes A, Melo E, Petrovski Z, Plechkova NV, Canongia Lopes JN, Seddon KR, Rebelo LPN (2008) On the self-aggregation and fluorescence quenching aptitude of surfactant ionic liquids. J Phys Chem B 112(29):8645–8650. https://doi.org/10.1021/jp802179j
14. Cornellas A, Perez L, Comelles F, Ribosa I, Manresa A, Teresa Garcia M (2011) Self-aggregation and antimicrobial activity of imidazolium and pyridinium based ionic liquids in aqueous solution. J Colloid Interface Sci 355(1):164–171. https://doi.org/10.1016/j.jcis.2010.11.063
15. Garcia TM, Ribosa I, Perez L, Manresa A, Comelles F (2013) Aggregation behavior and antimicrobial activity of ester-functionalized imidazolium- and pyridinium-based ionic liquids in aqueous solution. Langmuir 29(8):2536–2545. https://doi.org/10.1021/la304752e
16. Garcia MT, Ribosaa I, Perez L, Manresa A, Comelles F (2014) Self-assembly and antimicrobial activity of long-chain amide-functionalized ionic liquids in aqueous solution. Colloids Surf B Biointerfaces 123:318–325. https://doi.org/10.1016/j.colsurfb.2014.09.033
17. Sharma R, Kamal A, Kang TS, Mahajan RK (2015) Interactional behavior of polyelectrolyte poly sodium 4-styrene sulphonate (NaPSS) with imidazolium based surface active ionic liquids in aqueous medium. Phys Chem Chem Phys 17(36):23582–23594. https://doi.org/10.1039/C5CP02642C
18. Pal A, Yadav S (2016) Binding interaction between 1-octyl-3-methylimidazolium bromide and sodium polystyrene sulfonate in aqueous solution. Fluid Phase Equilib 412:71–78. https://doi.org/10.1016/j.fluid.2015.12.034
19. Zhang Q, Kang W, Sun D, Liu J, Wei X (2013) Interaction between cationic surfactant of 1-methyl-3-tetradecylimidazolium bromide and anionic polymer of sodium polystyrene sulfonate. Appl Surf Sci 279:353–359. https://doi.org/10.1016/j.apsusc.2013.04.105
20. Liu J, Zheng L, Sun D, Wei X (2010) Salt effect on the complex formation between 1-dodecyl-3-methylimidazolium bromide and sodium carboxymethylcellulose in aqueous solution. Colloids Surf A Physicochem Eng Asp 358(1-3):93–100. https://doi.org/10.1016/j.colsurfa.2010.01.034
21. Bandres I, Meler S, Giner B, Cea P, Lafuente C (2009) Aggregation behavior of pyridinium-based ionic liquids in aqueous solution. J Solut Chem 38(12):1622–1634. https://doi.org/10.1007/s10953-009-9474-4
22. Jiang Z, Li XF, Yang GF, Cheng L, Cai B, Yang Y, Dong J (2012) pH-responsive surface activity and solubilization with novel pyrrolidone-based Gemini surfactants. Langmuir 28(18):7174–7181. https://doi.org/10.1021/la3008156
23. Sastry NV, Vaghela NM, Macwan PM, Soni SS, Aswal VK, Gibaud A (2012) Aggregation behavior of pyridinium based ionic liquids in water–surface tension, ^{1}H NMR chemical shifts, SANS and SAXS measurements. J Colloid Interface Sci 371(1):52–61. https://doi.org/10.1016/j.jcis.2011.12.077
24. Dabholkar VV, Tripathi DR (2011) Synthesis and antibacterial activity of isochromene and isoquinoline derivative. J Heterocycl Chem 48(3):529–532. https://doi.org/10.1002/jhet.245
25. Lava K, Evrard Y, Hecke KV, Meervel LV, Binnemans K (2012) Quinolinium and isoquinolinium ionic liquid crystals. RSC Adv 2(21):8061–8070. https://doi.org/10.1039/c2ra21208k
26. Visser AE, Holbrey JD, Rogers RD (2001) Hydrophobic ionic liquids incorporating *N*-alkylisoquinolinium cations and their utilization in liquid–liquid separations. Chem Commun 23:2484–2485
27. Domańska U, Zawadzki M, Paduszyński K, Królikowski M (2012) Perturbed-chain SAFT as a versatile tool for thermodynamic modeling of binary mixtures containing isoquinolinium ionic liquids. J Phys Chem B 116(28):8191–8200. https://doi.org/10.1021/jp303988k
28. Domańska U, Zawadzki M, Lewandrowska A (2012) Effect of temperature and composition on the density, viscosity, surface tension, and thermodynamic properties of binary mixtures of *N*-octylisoquinoliniumbis{(trifluoromethyl)sulfonyl}imide with alcohols. J Chem Thermodyn 48:101–111. https://doi.org/10.1016/j.jct.2011.12.003
29. Domańska U, Zawadzki M, Królikowska M, Tshibangu MM, Ramjugernath D, Letcher TM (2011) Measurements of activity coefficients at infinite dilution of organic compounds and water in isoquinolinium-based ionic liquid [C_8iQuin][NTf_2] using GLC. J Chem Thermodyn 43(3):499–504. https://doi.org/10.1016/j.jct.2010.10.026
30. Domańska U, Zawadzki M, Królikowski M, Lewandrowska A (2012) Phase equilibria study of binary and ternary mixtures of {Noctylisoquinoliniumbis{(trifluoromethyl)sulfonyl}imide + hydrocarbon, or an alcohol, r water}. J Chem Thermodyn 181:63–71
31. Zhang X, Peng X, Ge L, Yu L, Liu Z, Guo R (2014) Micellization behavior of the ionic liquid lauryl isoquinolinium bromide in aqueous solution. Colloid Polym Sci 292(5):1111–1120. https://doi.org/10.1007/s00396-013-3151-2
32. Bakshi MS, Sachar S (2004) Surfactant polymer interactions between strongly interacting cationic surfactants and anionic polyelectrolytes from conductivity and turbidity measurements. Colloid Polym Sci 282(9):993–999. https://doi.org/10.1007/s00396-003-1022-y
33. Touhami Y, Rana D, Neale GH, Hornof V (2001) Study of polymer-surfactant interactions via surface tension measurements. Colloid Polym Sci 279(3):297–300. https://doi.org/10.1007/s003960000455
34. Staples E, Tucker I, Penfold J, Warren N, Thomas RK (2002) Organization of polymer−surfactant mixtures at the air−water interface: poly(dimethyldiallylammonium chloride), sodium dodecyl sulfate, and hexaethylene glycol monododecyl ether. Langmuir 18(13):5139–5146. https://doi.org/10.1021/la011863o
35. Goddard ED (2002) Polymer/surfactant interaction: interfacial aspects. J Colloid Interface Sci 256(1):228–235. https://doi.org/10.1006/jcis.2001.8066
36. Cervantes-Martínez A, Maldonado A (2007) Foaming behaviour of polymer–surfactant solutions. J Phys Condens Matter 19(24):246101–246107. https://doi.org/10.1088/0953-8984/19/24/246101
37. Pandey S, Bagwe RP, Shah DO (2003) Effect of counterions on surface and foaming properties of dodecyl sulfate. J Colloid Interface Sci 267(1):160–166. https://doi.org/10.1016/j.jcis.2003.06.001
38. Dong B, Zhao X, Zheng L, Zhang J, Li N, Inoue T (2008) Aggregation behavior of long-chain imidazolium ionic liquids in aqueous solution: micellization and characterization of micelle microenvironment. Colloids Surf A Physicochem Eng Asp 317(1-3):666–672. https://doi.org/10.1016/j.colsurfa.2007.12.001
39. Moroi Y (1992) Micelles: theoretical and applied aspects. Plenum Press, New York. https://doi.org/10.1007/978-1-4899-0700-4
40. Pal A, Yadav A (2015) Modulations in the aggregation behavior of ionic liquid 1-butyl-3-methylimidazolium octylsulfate in aqueous alcohol solutions. J Mol Liq 212:569–575. https://doi.org/10.1016/j.molliq.2015.10.009

41. Inoue T, Ebina H, Dong B, Zheng L (2007) Electrical conductivity study on micelle formation of long-chain imidazolium ionic liquids in aqueous solution. J Colloid Interface Sci 314(1):236–241. https://doi.org/10.1016/j.jcis.2007.05.052
42. Wang J, Wang H, Zhang S, Zhang H, Zhao Y (2007) Conductivities, volumes, fluorescence, and aggregation behavior of ionic liquids [C_4mim][BF_4] and [$C_n$mim]Br (n = 4, 6, 8, 10, 12) in aqueous solutions. J Phys Chem B 111(22):6181–6188. https://doi.org/10.1021/jp068798h
43. Wang J, Zhang L, Wang H, Wu C (2011) Aggregation behavior modulation of 1-dodecyl-3-methylimidazolium bromide by organic solvents in aqueous solution. J Phys Chem B 115(17):4955–4962. https://doi.org/10.1021/jp201604u
44. Singh T, Kumar A (2008) Self-aggregation of ionic liquids in aqueous media: a thermodynamic study. Colloids Surf A Physicochem Eng Asp 318(1-3):263–268. https://doi.org/10.1016/j.colsurfa.2007.12.043
45. Chen LG, Bermudez H (2012) Solubility and aggregation of charged surfactants in ionic liquids. Langmuir 28(2):1157–1162. https://doi.org/10.1021/la2040399
46. Rosen MJ (1988) Surfactant and interfacial phenomenon2nd edn. Wiley, New York
47. Tardani F, Mesa CL (2015) Titration of DNA/carbon nanotube complexes with double-chained oppositely charged surfactants. Nanomaterials (Basel) 5(2):722–736. https://doi.org/10.3390/nano5020722